CIELAB Color Space based High Resolution Satellite Image Segmentation using Modified Fuzzy C-Means Clustering

Ganesan P[1,*], V.Rajini[2], B.S.Sathish[1], Khamar Basha Shaik[1]

[1] Research Scholar, Sathyabama University, Sozhinganallur, Chennai, India.
[2] Professor, Dept.of Electrical and Electronics, SSN College of Engg, Chennai, India.

Abstract: This paper presented a novel approach for the segmentation of high resolution satellite images using the spatial information incorporated modified fuzzy c-means clustering algorithm. The images after preprocessing and geo referencing, the satellite images are available in RGB color space. In this device dependent and non uniform color space, the intensity and color information are mixed and also the effectiveness of the color information mainly depends upon the type of light sources used. So RGB color space is not preferred for the segmentation and pattern recognition. In this paper, this problem is solved by the application of perceptually uniform CIELab color space. Even though FCM algorithm is one of the efficient approaches for image segmentation, it doesn't give any spatial information which is important for clustering problems. In modified FCM clustering algorithm, the spatial information is incorporated as a function of the weighted sum of the membership function. Moreover, the noisy pixels can be eliminated by image enhancement process. The result and efficiency of the proposed approach is compared with other soft computing and non-soft computing methods.

Keywords: image segmentation; image enhancement; color space; color space; CIELab; RGB; FCM; clustering

1. Introduction

The images acquired from the satellite provide huge information but it is very difficult to process and retrieve the necessary hidden treasure without a suitable approach. Several methods have been proposed for extracting the necessary information from high resolution satellite images. These methods include Gabor filter [15], morphological operations [16], Markov random fields (MRF) [14], fuzzy [19], genetic algorithm [19,20], threshold, histogram, neural network [21,22], and split and merge. However, every method has its own advantages and limitations.

In the proposed approach, the high resolution satellite image is clustered using the spatial information incorporated modified fuzzy c-means clustering algorithm. The standard fuzzy c-means (FCM) clustering algorithm is one of the most efficient methods for image segmentation. However, it doesn't give any spatial information which is important for clustering problems [1]. In modified FCM clustering algorithm, the spatial information is incorporated as a function of the weighted sum of the membership function. The modified FCM clustering is clearly explained in section 2.

The satellite images after preprocessing and geo referencing are available in RGB color space. In this color space, the effectiveness of the color information, in the case of recognition and segmentation, mainly depends upon the type of light sources. This is the reason why RGB color space is not widely used for color information processing applications such as segmentation and pattern recognition. This problem can be solved by the application of perceptually uniform color spaces like CIE Lab or CIELuv [3,7].

CIELab color space is originally derived from CIEXYZ color space and defined by International Commission on Illumination (in French, Commission Internationale de l'Eclairage - CIE). This color space has three components or layers as L (lightness) and two color information components (a and b). The lightness L=0 indicates black and L=100 yields diffused white. The component a indicates the corresponding position in the color red-green as +127 represents pure red and a = -127 means pure green. Similarly, the component b indicates

(DOI: dx.doi.org/14.9831/1444-8939.2014/2-6/MAGNT.30)

the corresponding position in the color red-green as b=+127 indicates pure yellow and its negative denotes pure blue [5].

As compared to other color spaces, CIELab space is designed to approximate the human vision. In this perceptually uniform color space, the luminance component (L) closely matches the human perception of vision (lightness). The color balance corrections is easily performed by the adjusting the output curves in the other two components (a and b) of the CIELab system. Moreover, in other color spaces, the computation of distance between two colors is very difficult. In CIELab, this can easily be computed as the difference between two colors as human eye perception [6].

It is necessary to convert RGB to CIELab color space as per CCIR recommendation 709 to compute the correction matrices between the original and segmented image [9]. CIE Lab color space represents colors in the way that human eye perceives and permits the accurate and efficient representation at low cost [10].

The transformation of image from gamma corrected RGB color space to CIEXYZ color space is given in (1) (2) and (3)

$$X = 0.412453*R' + 0.35758*G' + 0.180423*B' \quad (1)$$

$$Y = 0.212671*R' + 0.71516*G' + 0.072169*B' \quad (2)$$

$$Z = 0.019334*R' + 0.119193*G' + 0.950227*B' \quad (3)$$

The transformation of image from CIEXYZ color space to CIELab color space is given in (4) (5) and (6)

$$L = 116\, f(Y/Yn) - 16 \quad (4)$$

$$a = 500[f(X/Xn) - f(Y/Yn)] \quad (5)$$

$$b = 200[f(Y/Yn) - f(Z/Zn)] \quad (6)$$

2. The Spatial information incorporated Modified Fuzzy C-Means Clustering

Fuzzy C-Means clustering (FCM), an iterative method, generates more than one optimal clusters by minimizing the objective function [13] which is given in (7)

$$J = \sum_{j=1}^{N} \sum_{i=1}^{c} U_{ij}^{m} \left\|X_j - V_i\right\|^2 \quad (7)$$

The degree of membership of data set X = {x_1, x_2... x_n} $= X_j$ can computed by (8) and i^{th} cluster centers can be calculated using (9)

$$U_{ij} = \sum_{k=1}^{c} \left\{\frac{\|X_j - V_i\|}{\|X_j - V_k\|}\right\}^{-2/m-1} \quad (8)$$

$$V_i = \frac{\sum_{j=1}^{n} (U_{ij})^m X_j}{\sum_{j=1}^{n} (U_{ij})^m} \quad (9)$$

Even though FCM algorithm is one of the efficient approaches for image segmentation, it has some significant drawbacks. Firstly, the conventional FCM method doesn't give any spatial information which is important for clustering problems [12]. Secondly, when the image pixel is incorporated with the noise pixels, the membership of fuzzy function can't be accurate and never correspond well to the degree of belonging of the data [2]. These drawbacks of conventional FCM are taken into consideration and incorporate the spatial information as a function of the weighted sum of the membership function in the neighborhood of each pixel under consideration [8,11].

$$S_{ij} = \sum_{k \in W(X_j)} U_{ik} \alpha_{k1} + \frac{\sum_{k \in (X_j)} U_{ik} \alpha_{k2}}{\sum_{t=1}^{c} \sum_{k \in W(X_j)} U_{tk}} \quad (10)$$

The new membership function after incorporating the spatial information is given by (11)

$$U_{ij\,(new)} = \frac{U_{ij}^{p} * S_{ij}^{q}}{\sum_{k=1}^{c} U_{kj}^{p} * S_{kj}^{q}} \quad (11)$$

In an image, every pixel has a weight (W_{ji}) in relation to every cluster.

$$W_{ji} = \frac{1}{1 + e^{-\left\{\frac{\|x_j - v_i\|^2}{\sum_{j=1}^{n} \|x_j - v_i\|^2 \left(\frac{c}{n}\right)}\right\}}} \quad (12)$$

(DOI: dx.doi.org/14.9831/1444-8939.2014/2-6/MAGNT.30)

Now, the objective function of the new and modified FCM clustering algorithm can be formulated as given in (13)

$$J_{Mod} = \sum_{k=1}^{n} \sum_{i=1}^{c} \left(U_{ik}^{m} W_{ji}^{m}\right) \|X_k - V_i\|^2 \quad (13)$$

The algorithm for modified fuzzy c means (MFCM) clustering for the segmentation of noisy satellite images is listed as follows.
Step 1: The test image is transformed to data matrix X
Step 2: Guess the number of clusters, c ($2 \leq c \leq n$), n is the length of the image data and fix the fuzziness parameter m > 1
Step 3: Compute the fuzzy partition matrix U_{ij} and, the i^{th} cluster center V_i using (8) and (9)
Step 4: Compute the spatial function S_{ij} and the weight function W_{ji} by using (10) and (12)
Step 5: The updated the new updated membership function is computed using (13)

3. Proposed Method for Segmentation

The proposed approach for the segmentation of satellite image based on modified fuzzy c-means clustering algorithm and CIElab color space is depicted in fig 1. The test image is acquired from the Landsat satellite (http://eros.usgs.gov/image gallery/image-week-2). The original image is sharpened using shaping algorithm in spatial domain. In this sharpening process, the kernel size of sobel is 5, low clip percentage is 0.01 and high clip percentage is 0.02. Then the sharpened image is smoothened using Gaussian filter if mask size 3.

The test image is in RGB color space. As already explained, In RGB color space, the effectiveness of the color information in the case of recognition and segmentation mainly depends upon the type of light sources. This is the reason why RGB color space is not widely used for color information processing applications such as segmentation and pattern recognition. This problem can be solved by the application of perceptually uniform color spaces like CIE Lab or CIELuv. The image in the RGB color space is first converted into CIEXYZ color space using linear transformation. CIEXYZ defined a 3D space where tristimulus values define a color. Then, the image in CIE XYZ color space is converted into CIELab color space. The modified fuzzy c-means clustering algorithm is applied to the CIELab image to do perform the clustering.

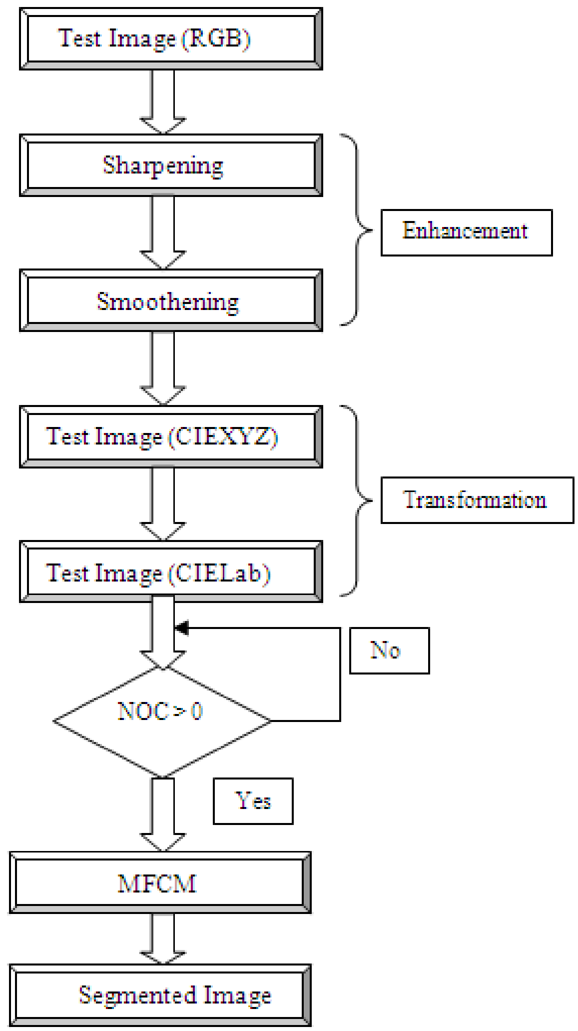

Fig. 1. Proposed approach for segmentation

4. Results and discussion

Fig 2(a) shows the satellite image of forest fires in Grampians National Park, Victoria, Australia which had acquired from Landsat 8 on 28-01-2014. The information collected from Landsat satellite images is valuable for mapping forest fires. Due to strong winds, hot and dry weather fires were rapidly spreaded to its larger extension. This forest fires completely destroyed 131000 acres of forest and created many environmental problems [17]. The

(DOI: dx.doi.org/14.9831/1444-8939.2014/2-6/MAGNT.30)

original image is sharpened using shaping algorithm in spatial domain. In this sharpening process, the kernel size of sobel is 5, low clip percentage is 0.01 and high clip percentage is 0.02. Then the sharpened image is smoothened using Gaussian filter if mask size 3.The sharpened and smoothened version of the test image is shown in fig 2(b) and 2(c) respectively.

The histogram of the original and sharpened image is shown in fig 3. This shows the difference between sharpened and unsharpened (test) images. The test image in RGB color space is transformed to CIEXYZ and then to CIELab color space as shown in fig 4. The three layers of test image (red, green and blue) and CIELab Image (luminance L, Chrominance a and b) is shown fig 5 and 6 respectively.

The modified FCM is applied to the CIELab color image for the segmentation based on colors. The clustering is performed using three different distance measures city block, squared Euclidean, and cosine. The color segmentation result for three clusters using city block, squared Euclidean and cosine distance measures is depicted in fig 7, 8 and 9 respectively. Similarly, the segmentation result based on color for four, five and six clusters using three different distance measures is illustrated in figure from 10 to 18.

Table 1 shows the segmentation result for three clusters using three different distance measures based on the proposed approach. The segmentation results for four, five and six clusters are depicted in table 2, 3 and 4 respectively. Table 5 illustrates the comparison of distances measures for various numbers of clusters. Fig 19 shows the graphical representation of the execution time and maximum number of iterations for different number of clusters. The segmentation result of various soft computing and non soft computing methods are illustrated in fig 20.

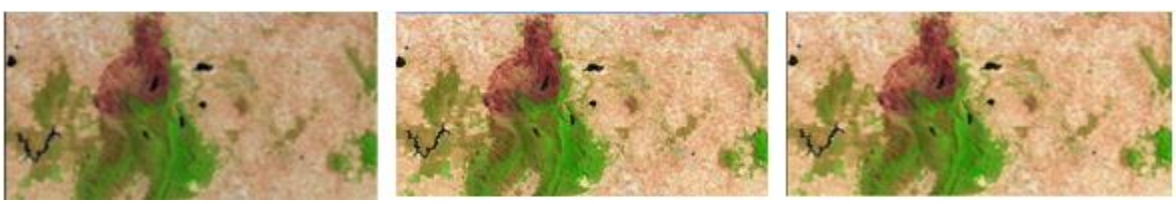

(a) Test Image (b) Sharpened Image (c) Smoothened Image

Fig. 2. Input image and its sharpened and smoothened version

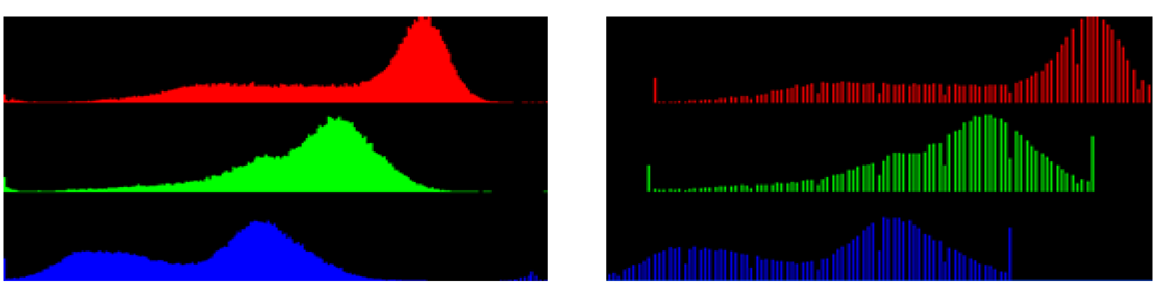

(DOI: dx.doi.org/14.9831/1444-8939.2014/2-6/MAGNT.30)

(a) Histogram of Test Image (b) Histogram of Sharpened Image

Fig. 3. The histogram of input and sharpened image

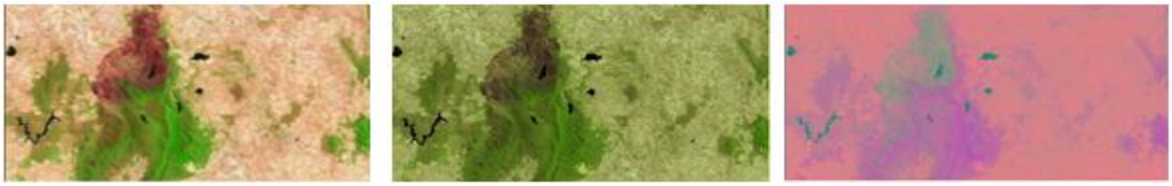

(a) RGB color space (b) CIE XYZ color space (c) CIE Lab color space

Fig. 4. Test image in three different color spaces

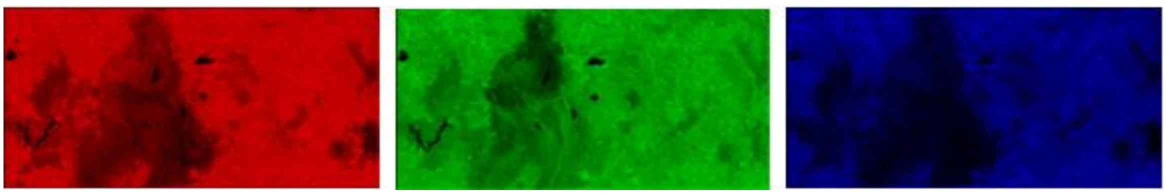

(a) Red layer (b) Green layer (c) Blue layer

Fig. 5. Three layers of RGB color space

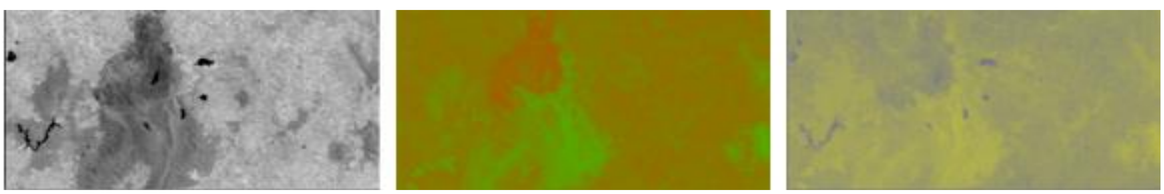

(a) L layer (b) a^* layer (c) b^* layer

Fig. 6. Three layers of CIELab color space

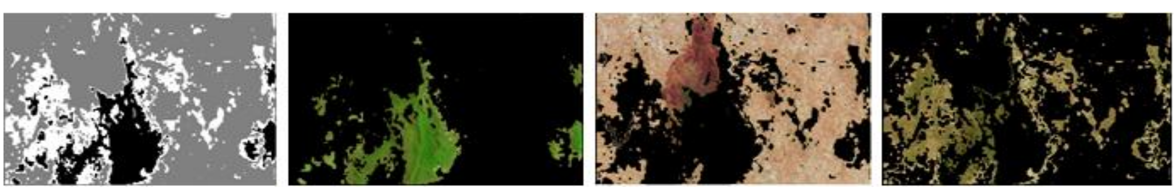

Fig. 7. The color segmentation result for three clusters (city block distance)

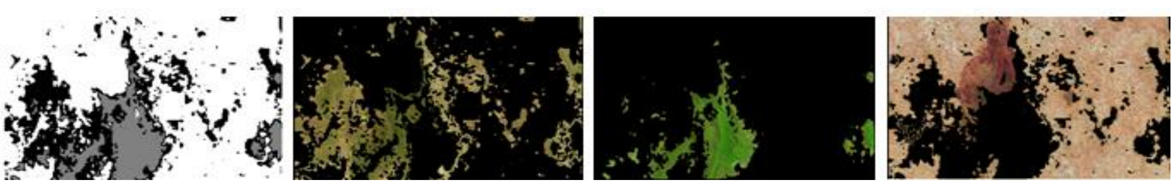

Fig. 8. The color segmentation result for three clusters (squared Euclidean distance)

(DOI: dx.doi.org/14.9831/1444-8939.2014/2-6/MAGNT.30)

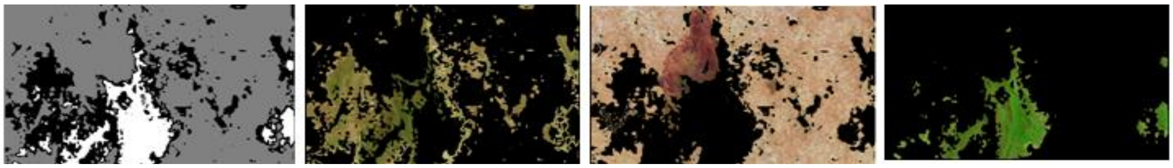

Fig. 9. The color segmentation result for three clusters (cosine distance)

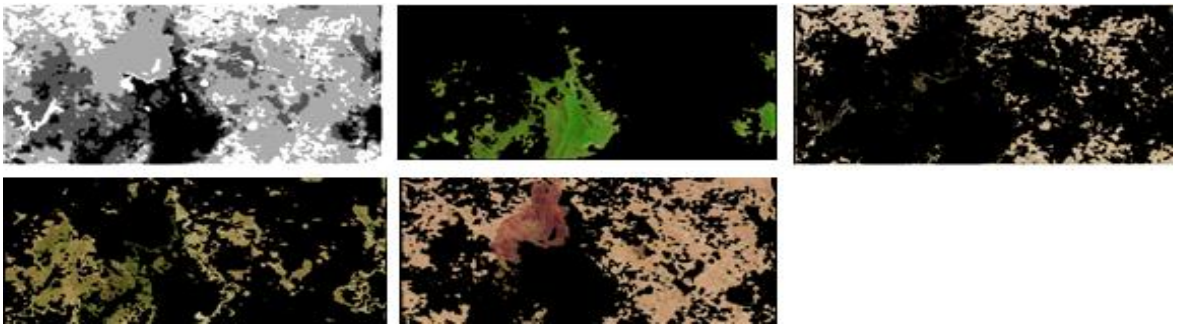

Fig. 10. The color segmentation result for four clusters (city block distance)

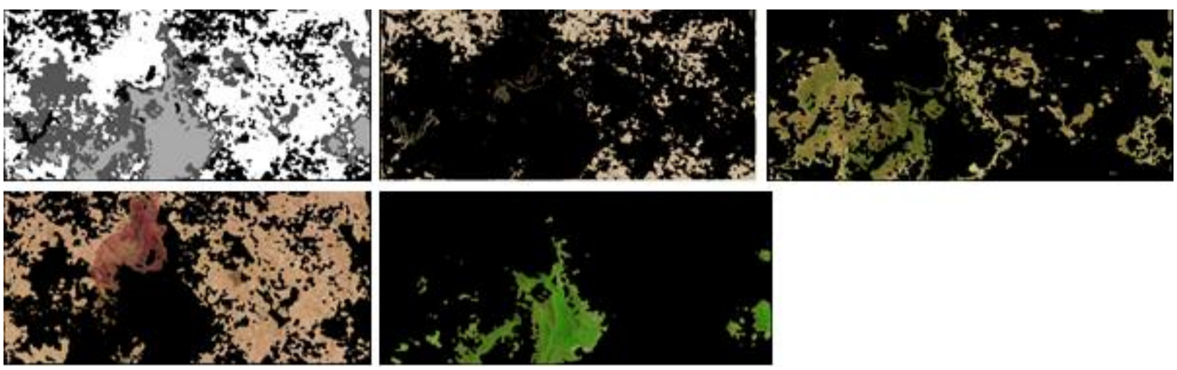

Fig. 11. The color segmentation result for four clusters (squared Euclidean distance)

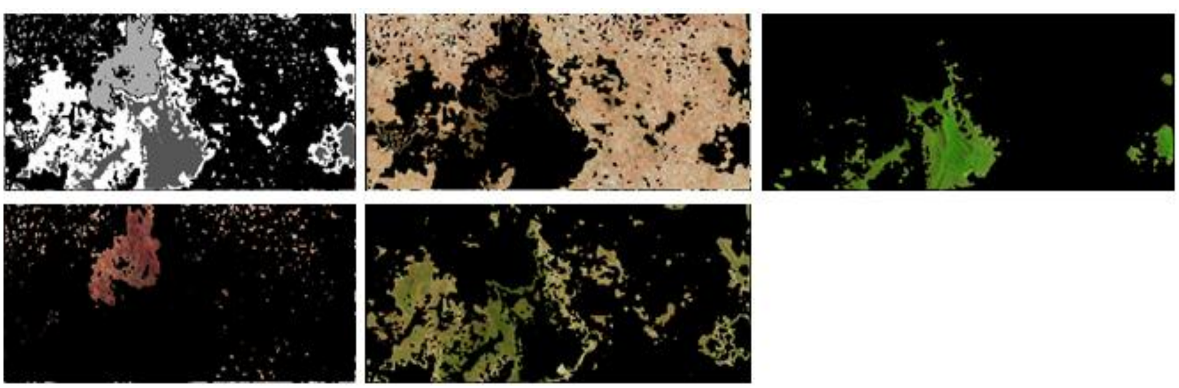

Fig. 12. The color segmentation result for four clusters (cosine distance)

(DOI: dx.doi.org/14.9831/1444-8939.2014/2-6/MAGNT.30)

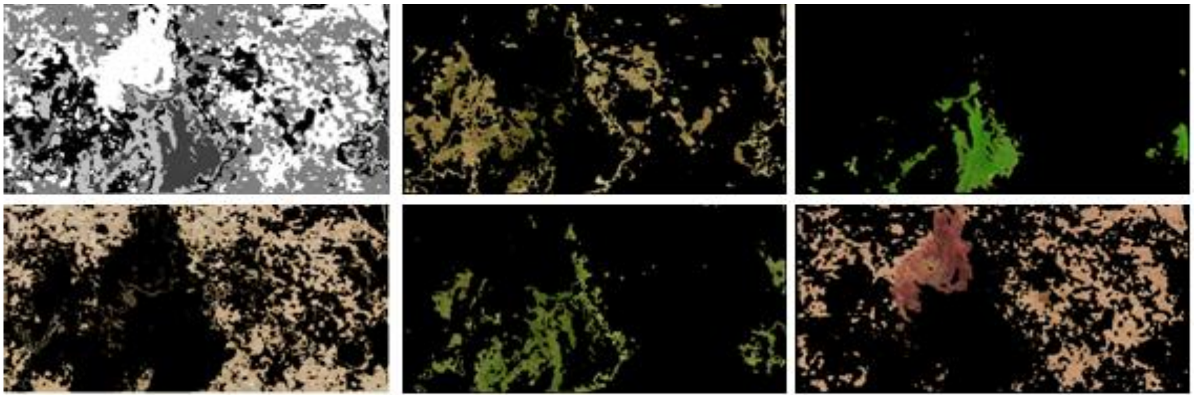

Fig. 13. The color segmentation result for five clusters (city block distance)

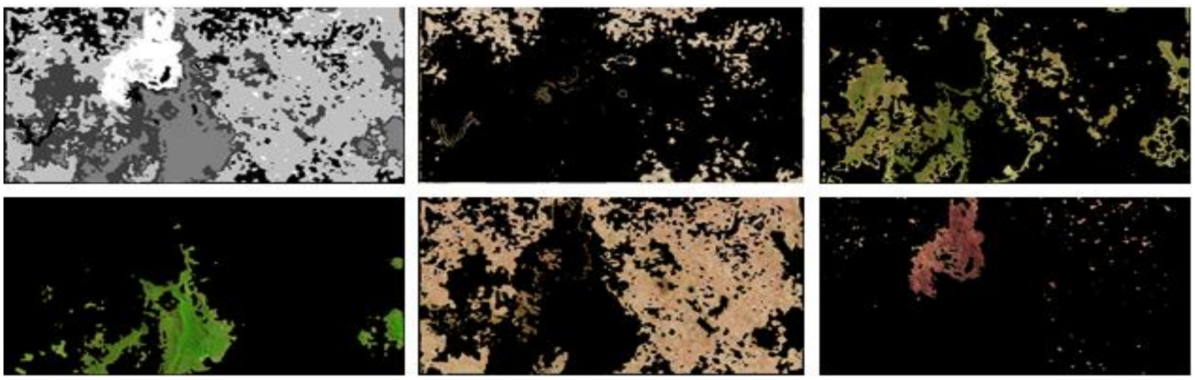

Fig. 14. The color segmentation result for five clusters (squared Euclidean distance)

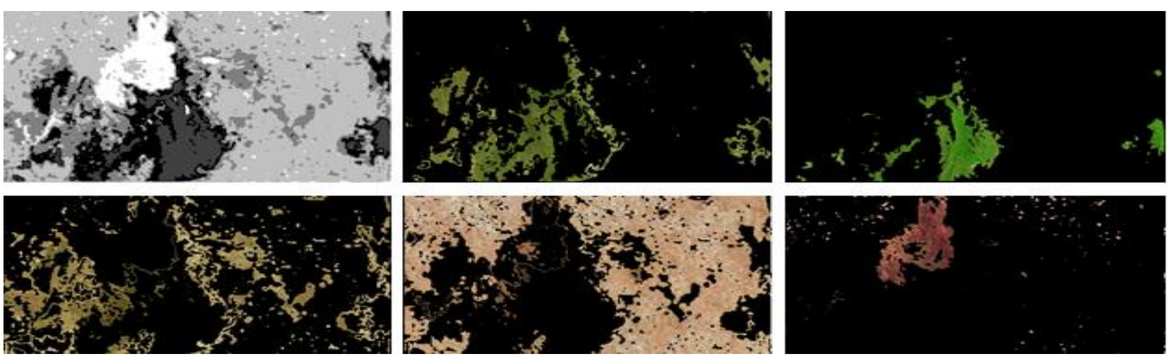

Fig. 15. The color segmentation result for five clusters (cosine distance)

(DOI: dx.doi.org/14.9831/1444-8939.2014/2-6/MAGNT.30)

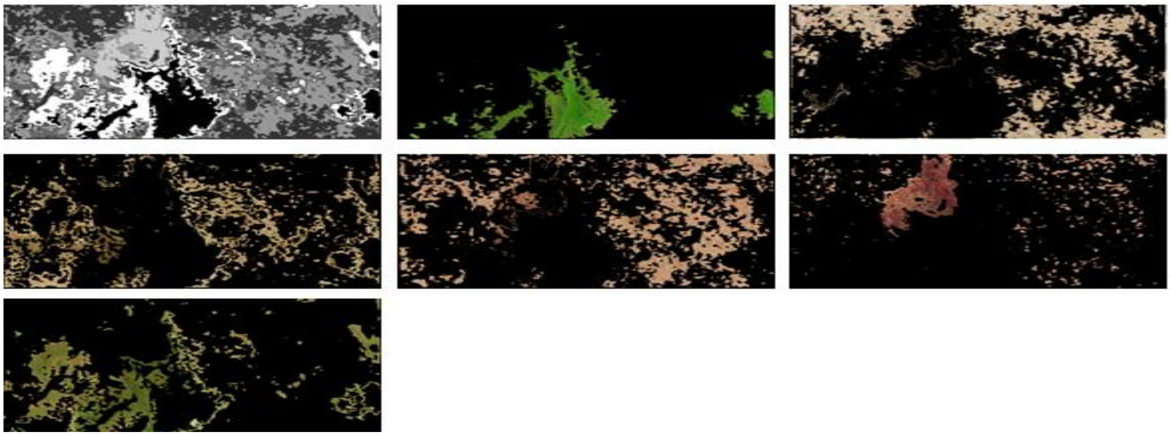

Fig. 16. The color segmentation result for six clusters (city block distance)

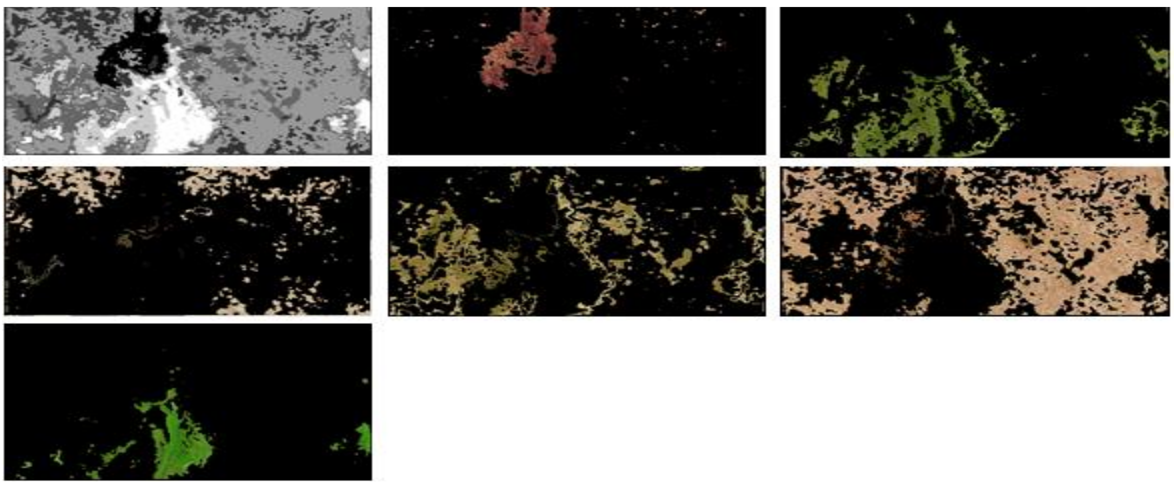

Fig. 17. The color segmentation result for six clusters (squared Euclidean distance)

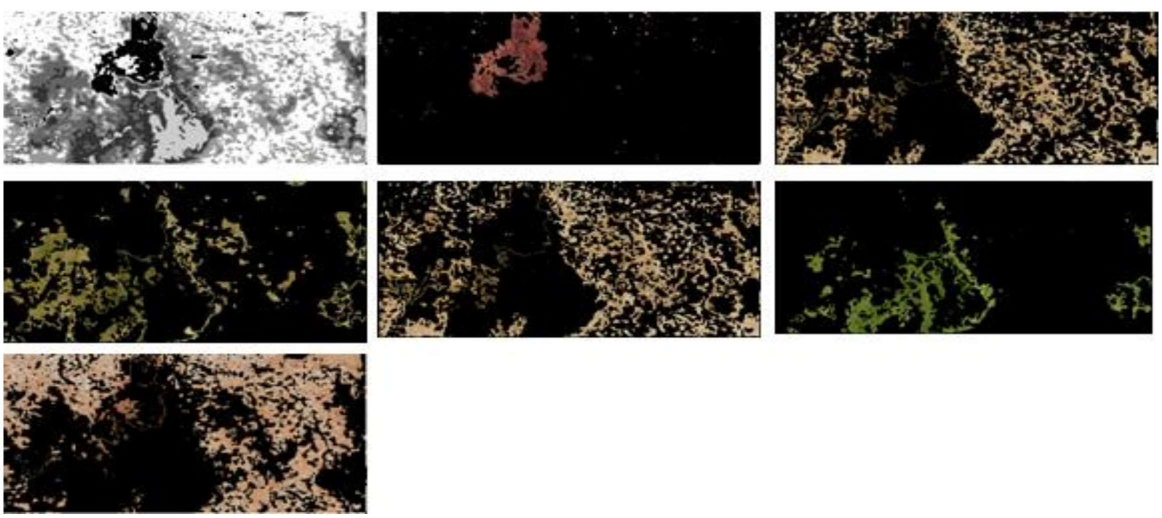

Fig. 18. The color segmentation result for six clusters (cosine distance)

(DOI: dx.doi.org/14.9831/1444-8939.2014/2-6/MAGNT.30)

Table 1. Segmentation result for three clusters using three different distance measures using proposed approach

	City block distance			Squared Euclidean distance			Cosine distance		
cluster	No. of iteration	Sum of distance	Cluster centers	No. of iteration	Sum of distance	Cluster centers	No. of iteration	Sum of distance	Cluster centers
1	8	679526	108,168	14	4.86215e+006	125.6,161.2	16	32.1896	0.6139,0.7888
2	8	642620	138,151	28	4.86394e+006	103.5,169.5	23	32.1896	0.6764,0.7359
3	9	645739	129,161	29	4.86394e+006	138.3,150.5	19	32.1896	0.5197,0.8853

Table 2. Segmentation result for four clusters using three different distance measures using proposed approach

	City block distance			Squared Euclidean distance			Cosine distance		
cluster	No. of iteration	Sum of distance	Cluster centers	No. of iteration	Sum of distance	Cluster centers	No. of iteration	Sum of distance	Cluster centers
1	6	623144	126,162	21	3.796e+006	132.7,146.2	25	21.2084	0.6690,0.7430
2	6	554855	105,169	22	3.814e+006	125.6,161.4	22	21.2084	0.5156,08558
3	10	555560	133,149	18	4.018e+006	103.5,169.5	20	21.2084	0.7120,0.7017
4	6	583440	140,153	23	3.771e+006	140.7,152.3	18	21.27	0.6075,0.7938

Table 3. Segmentation result for five clusters using three different distance measures using proposed approach

	City block distance			Squared Euclidean distance			Cosine distance		
cluster	No. of iteration	Sum of distance	Cluster centers	No. of iteration	Sum of distance	Cluster centers	No. of iteration	Sum of distance	Cluster centers
1	10	507084	127,162	23	2.968e+006	132.3,144.1	36	13.5176	0.5763,0.8168
2	10	503416	107,168	23	2.875e+006	124.5,161.7	26	13.5176	0.4976,0.8667
3	5	500587	142,152	13	2.873e+006	103.2,169.6	43	13.5176	0.6325,0.7742
4	15	507097	133,147	40	2.968e+006	138.1,153.2	19	13.5264	0.6732,0.7392
5	11	503190	137,153	16	2.873e+006	151.2,146.5	38	13.5176	0.7178,0.6958

(DOI: dx.doi.org/14.9831/1444-8939.2014/2-6/MAGNT.30)

Table 4. Segmentation result for six clusters using three different distance measures using proposed approach

	City block distance			Squared Euclidean distance			Cosine distance		
cluster	No. of iteration	Sum of distance	Cluster centers	No. of iteration	Sum of distance	Cluster centers	No. of iteration	Sum of distance	Cluster centers
1	8	448419	138,153	35	2.208e+006	151.6,146.1	30	9.43929	0.7217,0.6918
2	8	454762	133,147	19	2.208e+006	132.3,144.1	28	9.416	0.5622,0.8266
3	10	472839	120,164	20	2.464e+006	129.3,159.8	26	9.4163	0.6152,0.7881
4	11	460946	131,159	15	2.206e+006	138.8,152.7	29	9.43929	0.6567,0.7540
5	9	466452	102,170	18	2.207e+006	115.1,164.6	34	9.43929	0.4899,0.8721
6	11	457279	147,149	29	2.208e+006	98.19,171.9	25	9.4163	0.6797,07333

Fig. 19. The execution time (left) and maximum number of iterations (right) for different number of clusters

Table 5. The comparison of distances measures for various numbers of clusters

	Three Cluster		Four Cluster		Five Cluster		Six Cluster	
Distance Measure	Execution time	PSNR	Execution time	PSNR	Execution time	PSNR	Execution time	PSNR
City block	1.2636	14.88	1.3104	17.82	1.8720	26.88	2.5272	21.12
Sq. Euclidean	1.6068	16.62	1.6380	16.53	2.3868	17.34	3.1512	20.60
Cosine	1.435	15.09	1.5912	17.98	3.0420	22.79	3.9780	23.56

(DOI: dx.doi.org/14.9831/1444-8939.2014/2-6/MAGNT.30)

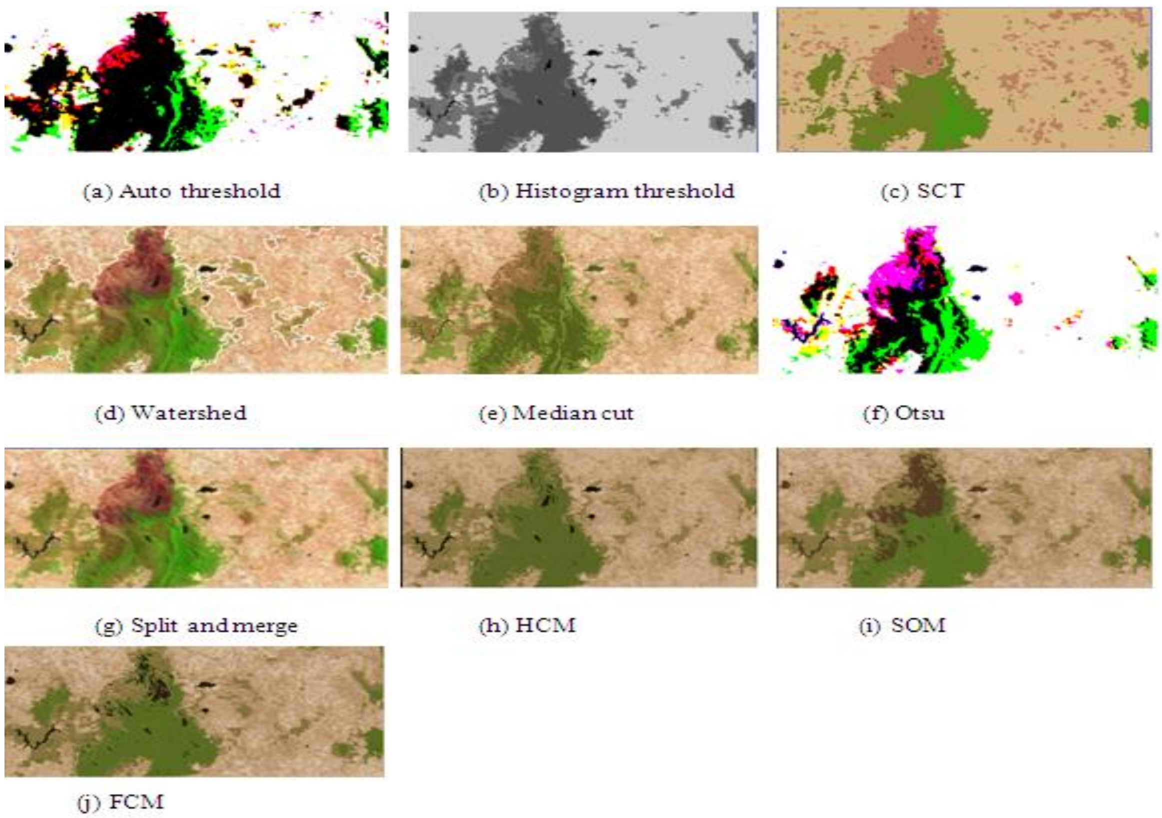

Fig. 20. The segmentation result using other methods

5. Conclusion

The high resolution satellite image segmentation based on modified fuzzy c-means clustering algorithm and CIELab color space is presented. In this paper, three important problems were identified and addressed to provide the optimal solution for the segmentation and clustering problems. Firstly, FCM is very insensitive to noise i.e., FCM treats noise pixel as image pixels. In this paper, the noise pixels can easily be eliminated by the image enhancement processes like sharpening and smoothening. Secondly, the non uniform RGB color space is transformed into perceptually uniform CIELab color space for the better representation of the image irrespective of display devices. Thirdly, the spatial information is very important for clustering problems but FCM doesn't give any spatial information. In the proposed approach, the spatial information is incorporated as a function of the weighted sum of the membership function. As compared to the result of other methods, the proposed approach is robust and efficient for the segmentation of satellite images.

References

1. Zhengjian Ding, Jin Sun, Yang Zang. FCM Image Segmentation algorithm based on color space and spatial information. International journal on computer and communication. Vol 2, No 1, 2013.
2. Ganesan P, Rajini V. A method to segment color images based on modified fuzzy-possibilistic-c-means clustering algorithm. Recent Advances in Space Technology Services and Climate Change (RSTSCC), 2010. IEEE; 2010.p.157-163.
3. Ganesan P, Rajini V. Segmentation and edge detection of color images using CIELAB color space and edge detectors. Emerging Trends in Robotics and Communication Technologies (INTERACT), 2010

(DOI: dx.doi.org/14.9831/1444-8939.2014/2-6/MAGNT.30)

International Conference on. IEEE; 2010.p.393-397.

4. Saha Sahaphong S. Unsupervised Image segmentation using automated Fuzzy C-Means", 7th IEEE Conference on computer and IT, Bangkok; 2007.p.690-694.
5. Corbalán M.CM, Millán, M. S. and Yzuel, M. J. Color pattern recognition with CIELab coordinates. Opt. Eng. vol. 41, no. 1, 2002. p. 130–138.
6. Hanbury A and Serra J. Mathematical morphology in the CIELAB space. Image Anal. Stereol. 21- 3, 2002.p. 201–206.
7. Thoonen G, Mahmood Z, Peeters S, Scheunders P. Multisource classification of color and hyper spectral images using color attribute profiles and composite decision fusion. Selected topics in applied earth observations and remote sensing, IEEE journal of, 5-2, 2012. p.510-521.
8. Ganesan P, Rajini V. Segmentation and Denoising of Noisy Satellite Images based on Modified Fuzzy C Means Clustering and Discrete Wavelet Transform for Information Retrieval. International Journal of Engineering & Technology; 2013.
9. Han Y. A Simple and Efficient Color Recovering System for Content Sharing Website. IEEE Transactions on Consumer Electronics. Vol. 56, No. 2, May 2010. p.863-869.
10. James M. Kasson and Wil Plouffe, "An Analysis of Selected Computer Interchange Color, Spaces," ACM Transactions on Graphics, Vol. 11, No. 4, pp.373-405, 1992.
11. Ganesan P, Rajini V. YIQ color space based satellite image segmentation using modified FCM clustering and histogram equalization. In Advances in Electrical Engineering (ICAEE), 2014 International Conference on, IEEE; 2014. p. 1-5.
12. Yang. Image segmentation by Fuzzy C Means Clustering Algorithm with a novel penalty term. Computing and Informatics, Vol. 26; 2007.p.17-31.
13. Ganesan P, Rajini V. Value based semi automatic segmentation of satellite images using HSV color space, histogram equalization and modified FCM clustering algorithm. In Green Computing, Communication and Conservation of Energy (ICGCE), 2013 International Conference on, IEEE; 2013. p. 77-82.
14. Poggi G, Scarpa G, Zerubia J B. Supervised segmentation of remote sensing images based on a tree-structured MRF model. *IEEE Trans.* Geosci. Remote Sens. vol. 43, no. 8, 2005. p. 1901–1911.
15. Bau T, Sarkar S, Healey G. Hyper spectral region classification using a three-dimensional gabor filterbank. IEEE Trans. Geosci. Remote Sens..vol. 48, no. 9, 2010. p.3457–3464.
16. Pesaresi M and Benediktsson J A. A new approach for the morphological segmentation of high-resolution satellite imagery. IEEE Trans.Geosci. Remote Sens., vol. 39, no. 2, 2001. p. 309–320.
17. http://eros.usgs.gov/image gallery/image-week-2
18. http://www.mathworks.com/
19. Awad M, Chehdi K, Nasri A. Multi-component image segmentation using a hybrid dynamic genetic algorithm and fuzzy C-means. IET Image Process. Vol. 3, Iss. 2, 2009. p. 52–62.
20. Lai C, Chang C.: 'A hierarchical genetic algorithm based approach for image segmentation'. Proc. IEEE International Conf. Networking, Sensing & Control, Taiwan, 2004, p. 1284–1288
21. Sergii Skakuna. Neural Network Approach To Flood Mapping Using Satellite Imagery. Computing and Informatics. Vol. 29, 2010. p.1013-1024
22. Janahiraman T V, and Win K. SOM Based Segmentation Method to Identify Water Region in LANDSAT Images. IJECCT.Vol. 2 (1), 2011. p.13-18.

(DOI: dx.doi.org/14.9831/1444-8939.2014/2-6/MAGNT.30)